

## Research Article

## Open Access

Jinn-Liang Liu\*, Dexuan Xie, and Bob Eisenberg

# Poisson-Fermi Formulation of Nonlocal Electrostatics in Electrolyte Solutions

<https://doi.org/10.1515/mlbmb-2017-0007>

Received June 2, 2017; accepted September 26, 2017

**Abstract:** We present a nonlocal electrostatic formulation of nonuniform ions and water molecules with interstitial voids that uses a Fermi-like distribution to account for steric and correlation effects in electrolyte solutions. The formulation is based on the volume exclusion of hard spheres leading to a steric potential and Maxwell's displacement field with Yukawa-type interactions resulting in a nonlocal electric potential. The classical Poisson-Boltzmann model fails to describe steric and correlation effects important in a variety of chemical and biological systems, especially in high field or large concentration conditions found in and near binding sites, ion channels, and electrodes. Steric effects and correlations are apparent when we compare nonlocal Poisson-Fermi results to Poisson-Boltzmann calculations in electric double layer and to experimental measurements on the selectivity of potassium channels for  $K^+$  over  $Na^+$ .

**Keywords:** Electrolytes; Ion channels; Poisson-Boltzmann; Poisson-Fermi

**MSC:** 35Q92, 53Z05, 65C20, 70E55, 92B05

## 1 Poisson-Fermi Theory

Continuum electrostatic theory is a fundamental tool for studying physical and chemical properties of electrolyte solutions in a wide range of applications in electrochemistry, biophysics, colloid science, and nanofluidics [1–8]. For over a century, a great deal of effort has been devoted to improving the Poisson-Boltzmann (PB) theory of continuum models for a proper description of steric (or finite size) and correlation (or nonlocal screening, polarization) effects in electrolytes [9–24]. We present a continuum model with Fermi-like distributions and global electrostatic screening of nonuniform ions and water molecules to describe the steric and correlation effects, respectively, in aqueous electrolyte solutions.

For an electrolytic system with  $K$  species of ions, the entropy model proposed in [20] treats all ions and water of any diameter as nonuniform hard spheres and regards the water as the  $(K + 1)^{\text{th}}$  species. It then includes the voids between these hard spheres as the  $(K + 2)^{\text{th}}$  species so that the total volume  $V$  of the system can be calculated exactly by the identity

$$V = \sum_{i=1}^{K+1} v_i N_i + V_{K+2}, \quad (1)$$

where  $V_{K+2}$  denotes the total volume of all the voids,  $v_i = 4\pi a_i^3/3$  that gives the volume of each sphere with radius  $a_i$ , and  $N_i$  is the total number of the  $i^{\text{th}}$  species particles. In the bulk solution, we have the bulk concentrations  $C_i^B = \frac{N_i}{V}$  and the bulk volume fraction of voids  $F^B = \frac{V_{K+2}}{V}$ . Dividing the volume identity (1)

\***Corresponding Author: Jinn-Liang Liu:** Institute of Computational and Modeling Science, National Tsing Hua University, Hsinchu 300, Taiwan, E-mail: jlliu@mx.nthu.edu.tw

**Dexuan Xie:** Department of Mathematical Sciences, University of Wisconsin-Milwaukee, Milwaukee, WI 53201-0413, USA, E-mail: dxie@uwm.edu

**Bob Eisenberg:** Department of Molecular Biophysics and Physiology, Rush University, Chicago, IL 60612 USA, E-mail: beisenbe@rush.edu

by  $V$ ,  $\Gamma^B = 1 - \sum_{i=1}^{K+1} v_i C_i^B$  is expressed in terms of nonuniform  $v_i$  and  $C_i^B$  for all particle species. If the system is spatially inhomogeneous with variable electric or steric fields, as in most biological and technological systems, the bulk concentrations then change to concentration functions  $C_i(\mathbf{r})$  that vary with positions, and differ from their constant values  $C_i^B$  at location  $\mathbf{r}$  in the solvent domain  $\Omega_s$ . Consequently, the void volume fraction becomes a function  $\Gamma(\mathbf{r}) = 1 - \sum_{i=1}^{K+1} v_i C_i(\mathbf{r})$  as well.

For an electrolyte in contact with electrodes or containing a charged protein, an electric field  $\mathbf{E}(\mathbf{r})$  in the solvent domain  $\Omega_s$  is generated by the electrodes, ionic (free) charges with a displacement field  $\mathbf{D}(\mathbf{r})$ , and bound charges of polar water with a polarization field  $\mathbf{P}(\mathbf{r})$ . In Maxwell's theory, these fields form a constitutive relation

$$\mathbf{D}(\mathbf{r}) = \epsilon_0 \mathbf{E}(\mathbf{r}) + \mathbf{P}(\mathbf{r}) \quad (2)$$

that yields the Maxwell's equation  $\nabla \cdot \mathbf{D}(\mathbf{r}) = \rho_I(\mathbf{r}) = \sum_{i=1}^K q_i C_i(\mathbf{r})$ ,  $\forall \mathbf{r} \in \Omega_s$ , where  $\epsilon_0$  is the vacuum permittivity and  $q_i$  is the charge on each  $i$  species ion [25, 26]. The electric field  $\mathbf{E}(\mathbf{r})$  is thus screened by water (in what might be called Bjerrum screening) and ions (in Debye screening) in a correlated manner that is usually characterized by a correlation (screening) length  $\lambda$  [4, 12, 27]. The screened force between two charges in ionic solutions (at  $\mathbf{r}$  and  $\mathbf{r}'$  in  $\Omega_s$ ) has been studied extensively in classical field theory and is often described by the screening kernel  $G(\mathbf{r} - \mathbf{r}') = \frac{e^{-|\mathbf{r}-\mathbf{r}'|/\lambda}}{4\pi|\mathbf{r}-\mathbf{r}'|}$  [1], which is called a Yukawa-type kernel in [4, 24, 28, 29], and satisfies the partial differential equation (PDE) [24, 28, 29]

$$-\Delta G(\mathbf{r} - \mathbf{r}') + \frac{1}{\lambda^2} G(\mathbf{r} - \mathbf{r}') = \delta(\mathbf{r} - \mathbf{r}'), \quad \mathbf{r}, \mathbf{r}' \in R^3 \quad (3)$$

in the whole space  $R^3$ , where  $\Delta = \nabla \cdot \nabla$  is the Laplace operator with respect to  $\mathbf{r}$  and  $\delta(\mathbf{r} - \mathbf{r}')$  is the Dirac delta function at  $\mathbf{r}'$ . The potential  $\tilde{\phi}(\mathbf{r})$  defined in  $\mathbf{D}(\mathbf{r}) = -\epsilon_s \epsilon_0 \nabla \tilde{\phi}(\mathbf{r})$  thus describes a local potential of free ions according to the Poisson equation

$$-\epsilon_s \epsilon_0 \nabla \cdot \nabla \tilde{\phi}(\mathbf{r}) = \rho_I(\mathbf{r}), \quad \forall \mathbf{r} \in \Omega_s, \quad (4)$$

where  $\epsilon_s$  is a dielectric constant in the solvent domain. This local potential does not deal with the long range correlations between different ions or between ions and polar water in high field or crowded conditions under which the size and valence of ions and the polarization of water play significant roles [4, 7, 12, 18–21, 27]. We introduce a global electric potential  $\phi(\mathbf{r})$  of the screened electric field  $\mathbf{E}(\mathbf{r})$  to deal with the correlation and polarization effects in electrolyte solutions. It is written as a convolution of the local potential  $\tilde{\phi}(\mathbf{r}')$  with the global screening kernel  $G(\mathbf{r} - \mathbf{r}')$ , i.e.,

$$\phi(\mathbf{r}) = \int_{R^3} \frac{1}{\lambda^2} G(\mathbf{r} - \mathbf{r}') \tilde{\phi}(\mathbf{r}') d\mathbf{r}'. \quad (5)$$

However, it would be too expensive to calculate  $\phi(\mathbf{r})$  using this equation. Multiplying Eq. (3) by  $\tilde{\phi}(\mathbf{r}')$  and then integrating over  $R^3$  with respect to  $\mathbf{r}'$  [24, 28, 29], we obtain

$$-\lambda^2 \Delta \phi(\mathbf{r}) + \phi(\mathbf{r}) = \tilde{\phi}(\mathbf{r}), \quad \mathbf{r} \in \Omega_s, \quad (6)$$

a PDE that approximates Eq. (5) in a sufficiently large domain  $\Omega_s$  with boundary conditions  $\phi(\mathbf{r}) = \tilde{\phi}(\mathbf{r}) = 0$  on  $\partial\Omega_s$  and describes the relation between global  $\phi(\mathbf{r})$  and local  $\tilde{\phi}(\mathbf{r})$  electric potentials. From Eqs. (4) and (6), we obtain the fourth-order PDE

$$\epsilon_s \epsilon_0 \lambda^2 \Delta(\Delta \phi(\mathbf{r})) - \epsilon_s \epsilon_0 \Delta \phi(\mathbf{r}) = \rho_I(\mathbf{r}), \quad \mathbf{r} \in \Omega_s. \quad (7)$$

Thus, when we set  $\mathbf{E}(\mathbf{r}) = -\nabla \phi(\mathbf{r})$ , we can use Eq. (2) to find the polarization field

$$\mathbf{P}(\mathbf{r}) = \epsilon_s \epsilon_0 \lambda^2 \nabla(\Delta \phi(\mathbf{r})) - (\epsilon_s - 1) \epsilon_0 \nabla \phi(\mathbf{r}). \quad (8)$$

If  $\lambda = 0$ , we recover the standard Poisson equation (4) and the approximate polarization  $\mathbf{P} = \epsilon_0(\epsilon_s - 1)\mathbf{E}$  with the electric susceptibility  $\epsilon_s - 1$  (and thus the dielectric constant  $\epsilon_s$ ) if water is treated as a time independent,

isotropic, and linear dielectric medium [26]. In this case, the field relation  $\mathbf{D} = \epsilon_s \epsilon_0 \mathbf{E}$  with the scalar constant permittivity  $\epsilon_s \epsilon_0$  is an approximation of the exact relation Eq. (2) due to the simplification of the dielectric responses of the medium material to the electric field  $\mathbf{E}$ .

We introduce a Gibbs free energy functional for the system as

$$\begin{aligned} F(\mathbf{C}, \phi) &= F_{el}(\mathbf{C}, \phi) + F_{en}(\mathbf{C}), \\ F_{el}(\mathbf{C}, \phi) &= \frac{1}{2} \int_{\Omega_s} \rho_1 \phi d\mathbf{r} = \frac{1}{2} \int_{\Omega_s} \rho_1 L^{-1} \rho_1 d\mathbf{r}, \\ F_{en}(\mathbf{C}) &= k_B T \int_{\Omega_s} \left\{ \sum_{i=1}^{K+1} C_i(\mathbf{r}) \left( \ln \frac{C_i(\mathbf{r})}{C_i^B} - 1 \right) + \frac{\Gamma(\mathbf{r})}{v_0} \left( \ln \frac{\Gamma(\mathbf{r})}{\Gamma^B} - 1 \right) \right\} d\mathbf{r}, \end{aligned} \quad (9)$$

where  $F_{el}(\mathbf{C}, \phi)$  is an electrostatic functional,  $F_{en}(\mathbf{C})$  is an entropy functional,  $\mathbf{C} = (C_1(\mathbf{r}), C_2(\mathbf{r}), \dots, C_{K+1}(\mathbf{r}))$ ,  $v_0 = (\sum_{i=1}^{K+1} v_i) / (K+1)$  an average volume, and  $L^{-1}$  is the inverse of the self-adjoint positive linear operator  $L = \epsilon_s \epsilon_0 \lambda^2 \Delta \Delta - \epsilon_s \epsilon_0 \Delta$  [24, 28, 29]. Taking the variations of  $F(\mathbf{C}, \phi)$  at  $\phi$  gives Eq. (7). Taking the variations of  $F(\mathbf{C}, \phi)$  at  $C_i(\mathbf{r})$  [24, 28, 29] yields Fermi-like distributions

$$C_i(\mathbf{r}) = C_i^B \exp \left( -\beta_i \phi(\mathbf{r}) + \frac{v_i}{v_0} S^{\text{trc}}(\mathbf{r}) \right), \quad S^{\text{trc}}(\mathbf{r}) = \ln \left( \frac{\Gamma(\mathbf{r})}{\Gamma^B} \right), \quad (10)$$

for all  $i = 1, \dots, K+1$  (ions and water), where  $\beta_i = q_i / k_B T$  with  $q_{K+1} = 0$ ,  $k_B$  is the Boltzmann constant, and  $T$  is an absolute temperature. The distribution is of Fermi type since it saturates. All concentration functions  $C_i(\mathbf{r}) < \frac{1}{v_i}$  [20], i.e.,  $C_i(\mathbf{r})$  cannot exceed the maximum value  $1/v_i$  for any arbitrary (or even infinite) potential  $\phi(\mathbf{r})$  in the domain  $\Omega_s$ . In these Fermi distributions, it is impossible for a particle volume  $v_i$  to be completely filled with particles, i.e., it is impossible to have  $v_i C_i(\mathbf{r}) = 1$  (and thus  $\Gamma(\mathbf{r}) = 0$ ) since that would yield  $S^{\text{trc}}(\mathbf{r}) = -\infty$  and hence  $v_i C_i(\mathbf{r}) = 0$ , a contradiction. For this reason, *we must include the void as a separate species if water and ions are all treated as hard spheres* [20]. Here we do represent water and ions as spheres. Our approach allows other shapes to be used as well but that is not done here.

The nonlocal Poisson-Fermi (PF) Eqs. (7) and (10) have new features, of some importance.

(i) The Fermi-like distribution of uniform spherical ions with voids in ionic liquids was first derived in [6, 12] using Bikerman's lattice model [30]. The entropy functional in [12] involves a reciprocal of a minimum volume  $v$  with a volume fraction  $\Phi$  that is an empirical fitting parameter and may have to be unrealistically large to fit experimental data in some applications [6]. It is shown in [20] that the entropy functional in [12] does not directly yield classical Boltzmann distributions  $C_i(\mathbf{r}) = C_i^B \exp(-\beta_i \phi(\mathbf{r}))$  as  $v \rightarrow 0$ . It can be easily seen from (10) that the entropy functional  $F_{en}(\mathbf{C})$  in Eq. (8) yields Boltzmann distributions as  $v_i \rightarrow 0$  for all  $i$ . Our derivation of  $F_{en}(\mathbf{C})$  does not employ any lattice models but simply uses the volume equation (1). The functional  $F_{en}(\mathbf{C})$  is a new modification of that in [20], where the classical Gibbs entropy is now generalized to include all species (ions, water, and voids) in electrolytes with the same entropy form. In fact, our  $\Gamma(\mathbf{r})$  is an analytical extension of the void fraction  $1 - \Phi$  in Bikerman's excess chemical potential [6], where all volume parameters  $v_i$  (including the bulk fraction  $\Gamma^B$ ) are physical not empirical. The adjustable parameter in our model is the correlation length  $\lambda \approx 2a_i$  depending on the ionic species  $i$  of interest [17, 20]. The PF model was first proposed in [6] without derivation and has been shown to produce results that are not only comparable to molecular dynamics (MD) simulation or experimental data but also provide insight into nonlinear properties of concentrated electrolytes and ionic liquids [31–34]. Here, we formally derive the PF model for general electrolytes using a hard-sphere instead of lattice model with the steric potential  $S^{\text{trc}}(\mathbf{r})$  first introduced in [17]. As compared with lattice models in [6] and demonstrated, for example, in [18, 20, 35], hard-sphere models significantly improve the agreement between simulation and experiment.

(ii) The fourth-order PDE (7) is similar to those in [12, 27] used in previous papers [17, 20]. However, the physical origin of the PDE is different. In [27], the global convolution is performed only on the charge density of point-like counter ions in contrast the convolution Eq. (5) to the potential  $\tilde{\phi}(\mathbf{r})$  by Eq. (4) that is generated by all spherical ions. In [12], a derivation for electrolytes or ionic liquids with steric effects is given from a

free energy function of a gradient expansion of nonlocal electrostatic energy in terms of  $\Delta\tilde{\phi}$ . Here, the fourth-order PDE is derived directly from Maxwell's equation with the Yukawa screening kernel. Our result does not depend on the convergence properties of an expansion of nonlocal electrostatic energy. The use of Green's function as a kernel in all previous works and the present work is the same although the convoluted function is quite different. From the definition of the displacement, electric, and polarization fields in Eq. (2), the association of the displacement field and free charges as in Eq. (4) [25, 26], and our derivation leading to the polarization field in Eq. (8), the new convolution formula (5) is more consistent with Maxwell's theory since our derivation is more concise without using the decomposition of long and short Coulomb interactions [27] or the gradient expansion of non-local electrostatic energy [12]. The decomposition approach requires a mean-field approximation and a strong-coupling expansion for the long-distance and short-distance interactions, respectively [27]. The fourth-order PDE is only the first order approximation of the energy expansion [12].

(iii) Eq. (7) defines a dielectric operator  $\hat{\epsilon} = \epsilon_s \epsilon_0 (1 - \lambda^2 \Delta)$  that in turn implicitly yields a dielectric function  $\tilde{\epsilon}(\mathbf{r})$  as an output of solving Eq. (7) [12, 20]. A physical interpretation of the operator was first introduced in [12] to describe the nonlocal permittivity in a correlated ionic liquid. The exact value of  $\tilde{\epsilon}(\mathbf{r})$  at any  $\mathbf{r} \in \Omega_s$  cannot be obtained from Eq. (7) but can be approximated by the simple formula  $\tilde{\epsilon}(\mathbf{r}) \approx \epsilon_0 + C_{\text{H}_2\text{O}}(\mathbf{r})(\epsilon_s - 1)\epsilon_0 / C_{\text{H}_2\text{O}}^{\text{B}}$  since the water density function  $C_{\text{H}_2\text{O}}(\mathbf{r}) = C_{K+1}(\mathbf{r})$  is an output of Eq. (10). This formula is only for visualizing (approximately) the profile of  $\hat{\epsilon}$  or  $\tilde{\epsilon}$ . It is not an input of calculation. The input is the operator  $\hat{\epsilon} = \epsilon_s \epsilon_0 (1 - \lambda^2 \Delta)$  (with its dependence on the input parameter the correlation length  $\lambda$ ). Therefore, the PF Eq. (7) accounts for electrostatic (ionic charges in Eq. (4)), correlation ( $\lambda$  in Eq. (5) and in  $\hat{\epsilon}$ ), polarization (Eq. (8)), nonlocal (Eq. (5)), and excluded volume (Eq. (1)) effects in electrolytes with Yukawa shielding with only one parameter  $\lambda$ .

(iv) The factor  $v_i/v_0$  multiplying  $S^{\text{trc}}(\mathbf{r})$  in Eq. (10) is a modification of the unity used in our previous work [20]. The steric energy  $-\frac{v_i}{v_0} S^{\text{trc}}(\mathbf{r}) k_B T$  [20] of a type  $i$  particle depends not only on the emptiness ( $I(\mathbf{r}) = 1 - \sum_{i=1}^{K+1} v_i C_i(\mathbf{r})$ ) (or equivalently crowding) at  $\mathbf{r}$  but also on the volume  $v_i$  of each type of particle. If all  $v_i$  are equal (and thus  $v_i = v_0$ ), then all particle species at any location  $\mathbf{r} \in \Omega_s$  have the same steric energy and the uniform particles are indistinguishable in steric energy. The steric potential is a mean-field approximation of Lennard-Jones (L-J) potentials that describe local variations of L-J distances (and thus empty voids) between every pair of particles. L-J potentials are highly oscillatory and extremely expensive and unstable to compute numerically. This dependence is worse than a nuisance. The L-J potentials are not well defined experimentally (e.g., the combining rules are not well defined, whether Lorentz-Berthelot or Kong rules are used). They are likely to depend on ionic species, concentration and perhaps other variables. It is dangerous to have a model that depends sensitively on parameters that are unknown experimentally.

(v) The global convolution in Eq. (5) may seem similar to those in [4, 24, 28, 29] but it is not. The Poisson equation (4) takes the place of the Fourier-Lorentzian (FL) equation — an integro-differential equation — in the previous work [4, 24, 28, 29] in which the local potential  $\tilde{\phi}(\mathbf{r}')$  in Eq. (5) is replaced by a global electric potential  $\Phi(\mathbf{r}')$ . Moreover, the factor  $1/\lambda^2$  in Eq. (5) is replaced by  $(\epsilon_s - \epsilon_\infty)/\lambda^2$ , where  $\epsilon_\infty$  and  $\lambda$  are both adjustable parameters. The choice of three parameters  $\epsilon_s$ ,  $\epsilon_\infty$ , and  $\lambda$  in the FL model is reduced to only one  $\lambda$  here.

## 2 Results

The nonlocal PF model is first compared with the modified PB model (mPB) of Borukhov et al. [36] in which ions are treated as cubes without considering void and correlation effects. The classical PB model (with  $\lambda = v_i = 0$  for all  $i$ , i.e., no size, void, and correlation effects) produces unphysically high concentrations of anions near the charged wall at  $x = 0$  as shown by the dashed curve in Fig. 1. The surface charge density is  $1e/(50\text{\AA}^2)$  in contact with a 0.1 M  $\text{C}_4\text{A}$  aqueous electrolyte, where the radius of both cations and anions is  $a = 4.65\text{\AA}$  in contrast to an edge length of  $7.5\text{\AA}$  of cubical ions in [36],  $e$  is the proton charge, and  $\epsilon_s = 80$ . The multivalent ions  $\text{A}^{4-}$  represent large polyanions adsorbed onto a charged Langmuir monolayer in experiments [36]. The dotted curve in Fig. 1 is similar to that of mPB in [36] and was obtained by the PF model with the size effect

but without voids and correlations, i.e.,  $\lambda = 0$ ,  $V_{K+2} = 0$  (no voids), and  $v_{K+1} = v_{H_2O} = 0$  (water is volumeless and hence  $\Gamma^B = 1 - \sum_{i=1}^K v_i C_i^B$  is the bulk water volume fraction). The voids ( $V_{K+2} \neq 0$ ) and water molecules ( $v_{H_2O} \neq 0$ ) have slight effects on  $A^{4-}$  concentration (because of saturation) and electric potential (because water and voids have no charges) profiles as shown by the thin solid curves in Figs. 1 and 2, respectively, when compared with the dotted curves. However, correlations (with  $\lambda = 1.6a$  [12]) of ions have significant effects on ion distributions as shown by the thick solid and dash-dotted curves in Fig. 1, where the Stern like layer is on the order of ionic radius  $a$  [37] and the overscreening layer [12] ( $C_{A^{4-}}(x) \approx 0$ ) of excess coions ( $C_{C^+}(x) > C_{C^+}^B = 0.4$  M) is about  $18 \text{ \AA}$  in thickness. The Stern like boundary layer is an output (not a prescribed condition) of our model and has no special significance here, except historical. Boundary layers are found frequently where physical properties change discontinuously or boundary conditions are imposed by mathematicians or physical systems. The electric potentials  $\phi(0) = 5.6$  at  $x = 0$  and  $\phi(11.5) = -1.97 k_B T/e$  in Fig. 2 obtained by PF with voids and correlations deviate dramatically from those by previous models for nearly 100% at  $x = 0$  (in the Stern layer) and 70% at  $x = 11.5 \text{ \AA}$  (in the screening layer) when compared with the maximum potential  $\phi(0) = 2.82 k_B T/e$  of previous models. The PF potential depth  $\phi(11.5) = -1.97 k_B T/e$  of the overscreening layer is very sensitive to the value of the correlation parameter  $\lambda = 1.6a$  since the depth tends to zero as  $a \rightarrow 0$ . The parameter value can only be justified with experimental or molecular dynamics (MD) data [17, 18, 20, 21].

The computational domain  $\{(x, y, z) : 0 \leq x \leq 40, -5 \leq y \leq 5, -5 \leq z \leq 5 \text{ \AA}\}$  for the results shown in Figs. 1 and 2 was chosen heuristically so that it is large enough to observe a zero Dirichlet boundary condition for  $\phi(\mathbf{r})$  at  $x = 40 \text{ \AA}$  within the accuracy to the third decimal place for five grid points near and at  $x = 40 \text{ \AA}$  for all potential profiles in Fig. 2. Zero Neumann boundary condition is given on the four walls adjacent to the charged wall ( $x = 0$ ) on which the condition is  $-\epsilon_s \nabla \phi \cdot \mathbf{n} = \sigma$  with  $\mathbf{n} = \langle -1, 0, 0 \rangle$  and  $\sigma = 1e/(50 \text{ \AA}^2)$ . The resulting water density (not shown) from Eq. (10) is approximately equal to the bulk density  $C_{H_2O}^2 = 55.5$  M at those grid points.

In implementation, the fourth-order PF equation is reduced to two second-order PDEs in [17] where boundary conditions for those equations can also be found. The computational efficiency of the PF model for solving linear systems is thus commensurable to that of standard or modified PB models. However, since the steric potential  $S^{\text{trc}}(\mathbf{r})$  in Eq. (10) depends sensitively on the unknown electric potential  $\phi(\mathbf{r})$  in a highly nonlinear manner and is obtained by solving the PF equation (7) coupled with Eq. (10) using exact or inexact Newton's iterative method [17], the computational cost of the PF model for nonlinear solver to achieve self-consistent convergence is in general much higher than that of PB models. For example, it took 42s of the CPU time for the PB profile (dashed curve) in Fig. 2 comparing with 1h 22min 50s (about 118 times costly) for the PF profile (thick solid curve) on a laptop with Intel Core i5-3230M CPU. The mesh size of the FD grid for this example is  $0.25 \text{ \AA}$  that yields a size of 270,641 for the matrix system. The error tolerance was set to 0.0001 and 0.005 for the linear and nonlinear solvers, respectively. It was very hard to converge for the PF model because the surface charge density  $\sigma$  is very high resulting in the saturation (i.e., the void fraction function  $\Gamma(\mathbf{r})$  in Eq. (10) is very close zero) of ionic concentrations as shown in Fig. 1 and the ion is very large resulting in strong nonlinearity in terms of the correlation parameter  $\lambda$ . Obviously, there is much room to improve the numerical method of the nonlinear solver used here and proposed in [17].

We next show the size effect of different ions with voids in a biological system. One of the main uses of ionic solution theory is the understanding of ions in protein channels that control a wide range of biological functions [7, 38, 39]. We consider the crystal structure of the potassium channel KcsA (PDB [40] ID 3F5W [41]) as shown in Fig. 3, where the spheres denote five specific cation binding sites (S0 to S4) [42]. The crystal structure with a total of  $N = 31268$  charged atoms is embedded in the protein domain  $\Omega_p$  while the binding sites are in the solvent domain  $\Omega_s$ . The exquisite selectivity of  $K^+$  (with  $a_{K^+} = 1.33 \text{ \AA}$ ) over other cations such as  $Na^+$  ( $a_{Na^+} = 0.95 \text{ \AA}$ ) by potassium channels is an intriguing quest in channology. It can be quantified by the free energy ( $G$ ) difference of  $K^+$  and  $Na^+$  in the pore and in the bulk solution [42–45]. Experimental measurements [43–45] showed that the relative free energy [42]

$$\Delta \Delta G(K^+ \rightarrow Na^+) = [G_{\text{pore}}(Na^+) - G_{\text{bulk}}(Na^+)] - [G_{\text{pore}}(K^+) - G_{\text{bulk}}(K^+)] \quad (11)$$

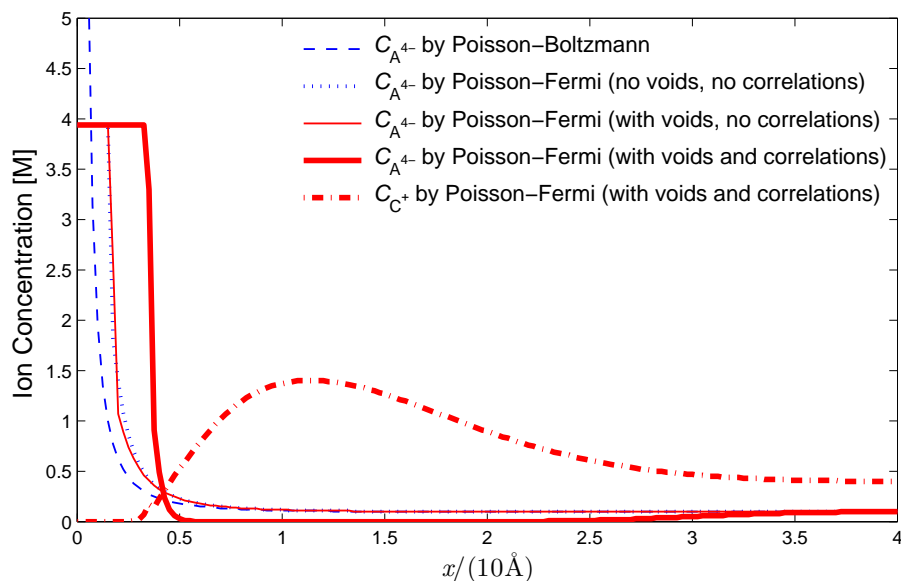


**Figure 1:** Concentration profiles of anions  $C_{A^{4-}}(x)$  and cations  $C_{C^+}(x)$  obtained by various models in a  $C_4A$  electrolyte solution with a positively charged surface at  $x = 0$ .

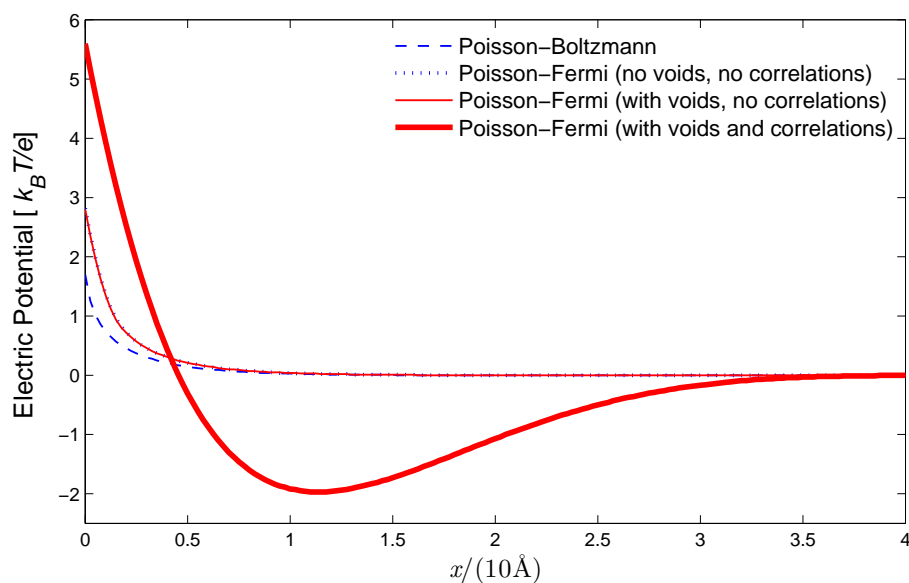


**Figure 2:** Electric potential profiles  $\phi(x)$ .

is greater than zero in the order of 5-6 kcal/mol unfavorable for  $Na^+$ . The electric and steric potentials at the binding site S2 (as considered in [42]) can be calculated on the atomic scale using the following algebraic formulas

$$\phi_{S2} = \frac{1}{4\pi\epsilon_0} \left( \frac{1}{6} \sum_{k=1}^6 \sum_{j=1}^N \frac{q_j}{\epsilon_p(r)|c_j - A_k|} + \frac{q_{S2}}{\epsilon_b a_{S2}} \right), \quad S_{S2}^{trc} = \ln \frac{1 - \frac{V_{S2}}{V_B}}{\Gamma^B}, \quad (12)$$

where  $S2 = Na^+$  or  $K^+$  (the site is occupied by a  $Na^+$  or a  $K^+$ ),  $q_j$  is the charge on the atom  $j$  in the protein given by PDB2PQR [46],  $\epsilon_p(r) = 1 + 77r/(27.7 + r)$  [47],  $r = |c_j - c_{S2}|$ ,  $c_j$  is the center of atom  $j$ ,  $A_k$  is one of six symmetric surface points on the spherical  $S2$ ,  $\epsilon_b = 3.6$ , and  $V_{S2} = 1.5V_{K^+}$  is a volume containing the ion at

S2. The crucial parameter in (12) is the ionic radius  $a_{S2} = 0.95$  or  $1.33 \text{ \AA}$  (also in  $|c_j - A_k|$ ) that affects  $\phi_{S2}$  very strongly but  $S_{S2}^{\text{trc}}$  weakly. We obtained  $\Delta\Delta G = 5.26 \text{ kcal/mol}$  in accord with the MD result  $5.3 \text{ kcal/mol}$  [42], where  $G_{\text{pore}}(\text{Na}^+) = 4.4$ ,  $G_{\text{bulk}}(\text{Na}^+) = -0.26$ ,  $G_{\text{pore}}(\text{K}^+) = -0.87$ ,  $G_{\text{bulk}}(\text{K}^+) = -0.27 \text{ kcal/mol}$ ,  $\phi_{\text{Na}^+} = 7.5 k_B T/e$ ,  $\frac{V_{\text{Na}^+}}{V_0} S_{\text{Na}^+}^{\text{trc}} = 0.23$ ,  $\phi_{\text{K}^+} = -1.93 k_B T/e$ ,  $\frac{V_{\text{K}^+}}{V_0} S_{\text{K}^+}^{\text{trc}} = -0.59$ , and  $C_{\text{Na}^+}^{\text{B}} = C_{\text{K}^+}^{\text{B}} = 0.4 \text{ M}$ .

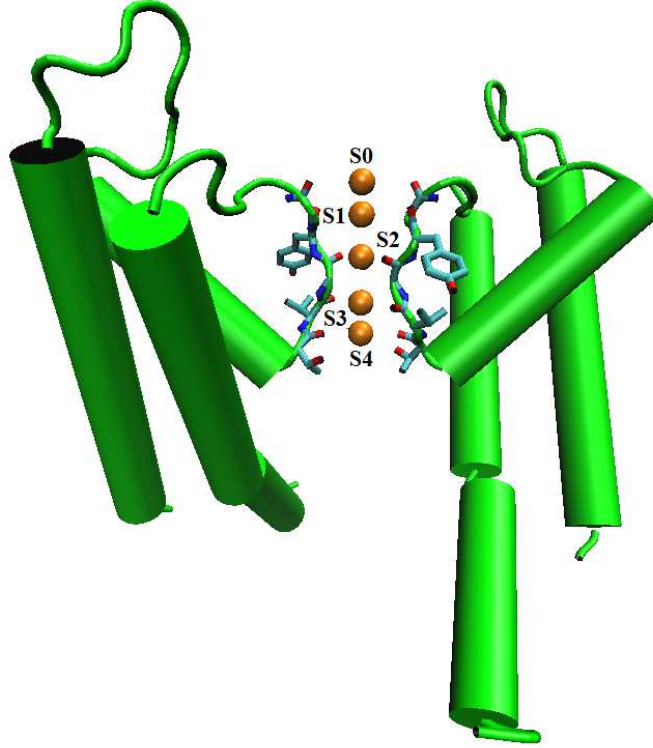


**Figure 3:** The crystal structure of the  $\text{K}^+$  channel KcsA (PDB ID 3F5W) [41] with five cation binding sites S0, S1, S2, S3, and S4 [42] marked by spheres.

For the above results, the bulk energies  $G_{\text{bulk}}(\text{Na}^+)$  and  $G_{\text{bulk}}(\text{K}^+)$  were obtained from the experimental results in [48]. The pore energies  $G_{\text{pore}}(\text{Na}^+)$  and  $G_{\text{pore}}(\text{K}^+)$  were obtained by the formula  $G_{\text{pore}}(S2) = q_{S2}\phi_{S2} - \frac{V_{S2}}{V_0} S_{S2}^{\text{trc}} k_B T$ , where S2 denotes  $\text{Na}^+$  or  $\text{K}^+$  and  $T = 298.15$ . The values of  $\phi_{S2}$  (i.e.  $\phi_{\text{Na}^+}$  and  $\phi_{\text{K}^+}$ ) and  $S_{S2}^{\text{trc}}$  ( $S_{\text{Na}^+}^{\text{trc}}$  and  $S_{\text{K}^+}^{\text{trc}}$ ) in  $G_{\text{pore}}(S2)$  were obtained using the equations in (12) with  $a_{S2} = 0.95$  ( $\text{Na}^+$ ) or  $1.33 \text{ \AA}$  ( $\text{K}^+$ ). The electric potential  $\phi_{S2}$  is generated by the charges  $q_j$  of all  $N = 31268$  atoms in the protein and the charge  $q_{S2}$  in the bound ion  $\text{Na}^+$  or  $\text{K}^+$  at S2. The steric potential  $S_{S2}^{\text{trc}}$  depends on the volume of the bound ion  $\text{Na}^+$  or  $\text{K}^+$  and the assumed volume  $V_{S2}$  of the binding site, which is adjustable. However, a slight change of  $V_{S2}$  does not affect significantly the steric energy difference between  $\text{Na}^+$  and  $\text{K}^+$  as shown by the steric formula in (12). Therefore, the change does not alter significantly the selectivity result obtained from Eq. (11). Other values (not shown) of  $\phi_{S_i}$  at other sites  $i = 0, 1, 3,$  and  $4$  can be calculated in the same way. These  $\phi_{S_i}$  values in the filter domain  $\Omega_f$  containing the five binding sites in Fig. 3 can be used as Dirichlet boundary data for the PF model (7) in the rest of the solvent domain  $\Omega_s/\Omega_f$  [49] to obtain a continuous electric potential function  $\phi(\mathbf{r})$  (not shown) in the whole domain  $\Omega = \Omega_s \cup \Omega_p$ , where  $\Omega_p$  denotes the domain of the protein and the membrane. Note that another Poisson equation is defined in  $\Omega_p$  and some conditions for  $\phi(\mathbf{r})$  should be imposed on the interface  $\partial\Omega_p$  between  $\Omega_s$  and  $\Omega_p$ . We refer to [17, 49] for more details on the model formulation and numerical methods.

### 3 Conclusion

In summary, a nonlocal Poisson-Fermi model is proposed to describe global electrostatic and steric effects that play a significant role of ionic activities in electrolyte solutions especially in high field or large concentration conditions. The model is based on Maxwell's field theory and nonuniform hard spheres of all ions and water molecules with interstitial voids. The Fermi-like distribution formula can describe the distribution of nonuniform spherical ions and water molecules with interstitial voids. The steric potential is a mean-field description of Lennard-Jones potentials between particles. Poisson's equation is self-consistent with Fermi distributions and global electrostatics. The present theory can be used to describe complex functions of biological or chemical structures on both atomic and macroscopic scales. Comparisons with experimental data are promising but incomplete.

This work was partially supported by the Ministry of Science and Technology, Taiwan (MOST 105-2115-M-007-016-MY2 to J.-L. Liu) and the National Science Foundation, USA (DMS-1226259 to D. Xie). We thank the Mathematical Biosciences Institute at the Ohio State University, USA for support for our visits and get together in Columbus in the fall of 2015.

### References

- [1] K. J. Laidler, J. H. Meiser, and B. C. Sanctuary, *Physical Chemistry* (Houghton Mifflin Co., Boston, 2003).
- [2] B. Hille, *Ionic Channels of Excitable Membranes* (Sinauer Associates Inc., Sunderland, MA, 2001); J. Zheng and M. C. Trudeau, *Handbook of ion channels* (CRC Press, 2015).
- [3] M. Boström, D. R. M. Williams, and B. W. Ninham, Specific ion effects: why DLVO theory fails for biology and colloid systems, *Phys. Rev. Lett.* **87**, 168103 (2001).
- [4] A. Hildebrandt, R. Blossey, S. Rjasanow, O. Kohlbacher, and H.-P. Lenhof, Novel formulation of nonlocal electrostatics, *Phys. Rev. Lett.* **93**, 108104 (2004).
- [5] A. Abrashkin, D. Andelman, and H. Orland, Dipolar Poisson-Boltzmann equation: ions and dipoles close to charge interfaces, *Phys. Rev. Lett.* **99**, 077801 (2007).
- [6] M. Z. Bazant, M. S. Kilic, B. D. Storey, and A. Ajdari, Towards an understanding of induced-charge electrokinetics at large applied voltages in concentrated solutions, *Adv. Coll. Interf. Sci.* **152**, 48-88 (2009).
- [7] B. Eisenberg, Crowded charges in ion channels, in *Advances in Chemical Physics*, S. A. Rice, Ed., John Wiley & Sons, Inc. **148**, 77-223 (2011).
- [8] G.-W. Wei, Q. Zheng, Z. Chen, and K. Xia, Variational multiscale models for charge transport, *SIAM Rev.* **54**, 699-754 (2012).
- [9] P. Attard, Electrolytes and the electric double layer, *Adv. Chem. Phys.* **92**, 1-159 (1996).
- [10] V. Vlatchy, Ionic effects beyond Poisson-Boltzmann theory, *Annu. Rev. Phys. Chem.* **50**, 145-165 (1999).
- [11] P. Grochowski and J. Trylska, Continuum molecular electrostatics, salt effects and counterion binding—A review of the Poisson-Boltzmann model and its modifications, *Biopolymers* **89**, 93-113 (2008).
- [12] M. Z. Bazant, B. D. Storey, and A. A. Kornyshev, Double layer in ionic liquids: Overscreening versus crowding, *Phys. Rev. Lett.* **106**, 046102 (2011).
- [13] Y. K. Hyon, B. Eisenberg, and C. Liu, A mathematical model for the hard sphere repulsion in ionic solutions, *Commun. Math. Sci.* **9**, 459-475 (2011).
- [14] B. Lu and Y. C. Zhou, Poisson-Nernst-Planck equations for simulating biomolecular diffusion-reaction processes II: Size effects on ionic distributions and diffusion-reaction rates, *Biophys. J.* **100**, 2475-2485 (2011).
- [15] B. Eisenberg, Ionic interactions are everywhere, *Physiol.* **28**, 28-38 (2013).
- [16] B. Eisenberg, Interacting ions in Biophysics: Real is not ideal, *Biophys. J.* **104**, 1849-1866 (2013).
- [17] J.-L. Liu, Numerical methods for the Poisson-Fermi equation in electrolytes, *J. Comput. Phys.* **247**, 88-99 (2013).
- [18] J.-L. Liu and B. Eisenberg, Correlated ions in a calcium channel model: a Poisson-Fermi theory, *J. Phys. Chem. B* **117**, 12051-12058 (2013).
- [19] J.-L. Liu and B. Eisenberg, Analytical models of calcium binding in a calcium channel, *J. Chem. Phys.* **141**, 075102 (2014).
- [20] J.-L. Liu and B. Eisenberg, Poisson-Nernst-Planck-Fermi theory for modeling biological ion channels, *J. Chem. Phys.* **141**, 22D532 (2014).
- [21] J.-L. Liu and B. Eisenberg, Numerical methods for a Poisson-Nernst-Planck-Fermi model of biological ion channels, *Phys. Rev. E* **92**, 012711 (2015).
- [22] T.-C. Lin and B. Eisenberg, A new approach to the Lennard-Jones potential and a new model: PNP-steric equations, *Commun. Math. Sci.* **12**, 149-173 (2014).



- [23] D. Chen, A new Poisson-Nernst-Planck model with ion-water interactions for charge transport in ion channels, *Bull. Math. Biol.* **78**, 1703-1726 (2016).
- [24] D. Xie, J.-L. Liu, and B. Eisenberg, Nonlocal Poisson-Fermi model for ionic solvent, *Phys. Rev. E* **94**, 012114 (2016).
- [25] J. D. Jackson, *Classical Electrodynamics* (Wiley, 1999).
- [26] A. Zangwill, *Modern Electrodynamics* (Cambridge University Press, New York, 2013).
- [27] C. D. Santangelo, Computing counterion densities at intermediate coupling, *Phys. Rev. E* **73**, 041512 (2006).
- [28] D. Xie, Y. Jiang, P. Brune, and L. R. Scott, A fast solver for a nonlocal dielectric continuum model, *SIAM J. Sci. Comput.*, **34**, B107-B126 (2012).
- [29] D. Xie and H. W. Volkmer, A modified nonlocal continuum electrostatic model for protein in water and its analytical solutions for ionic Born models, *Commun. Comput. Phys.* **13**, 174-194 (2013).
- [30] J. J. Bikerman, Structure and capacity of electrical double layer, *Philos. Mag.* **33**, 384-397 (1942).
- [31] B. D. Storey and M. Z. Bazant, Effects of electrostatic correlations on electrokinetic phenomena, *Phys. Rev. E* **86**, 056303 (2012).
- [32] X. Jiang et al., Dynamics of electrical double layer formation in room-temperature ionic liquids under constant-current charging conditions, *J. Phys.: Condens. Matter* **26**, 284109 (2014).
- [33] A. Yochelis, Transition from non-monotonic to monotonic electrical diffuse layers: impact of confinement on ionic liquids, *Phys. Chem. Chem. Phys.* **16**, 2836-2841 (2014).
- [34] A. Yochelis, M. B. Singh, I. Visoly-Fisher, Coupling bulk and near-electrode interfacial nanostructuring in ionic liquids, *Chem. Mater.* **27**, 4169-4179 (2015).
- [35] B. Giera et al., Model-free test of local-density mean-field behavior in electric double layers, *Phys. Rev. E* **88**, 011301 (2013).
- [36] I. Borukhov, D. Andelman, and H. Orland, Steric effects in electrolytes: A modified Poisson-Boltzmann equation, *Phys. Rev. Lett.* **79**, 435-438 (1997).
- [37] O. Stern, Zur theorie der elektrolytischen doppelschicht, *Z. Elektrochem.* **30**, 508-516 (1924).
- [38] E. Neher, Ion channels for communication between and within cells, in *Nobel Lecture, Physiology or Medicine 1991-1995*, N. Ringertz, Ed., World Scientific, Singapore, 10-25 (1997).
- [39] J. Zheng and M. C. Trudeau, *Handbook of Ion Channels*, CRC Press, 2015.
- [40] H. M. Berman et al., The protein data bank, *Nucleic Acids Res.* **28**, 235-242 (2000).
- [41] L. G. Cuello et al., Structural mechanism of C-type inactivation in K<sup>+</sup> channels, *Nature* **466**, 203-208 (2010).
- [42] S. Y. Noskov, S. Berneche, and B. Roux, Control of ion selectivity in potassium channels by electrostatic and dynamic properties of carbonyl ligands, *Nature* **431**, 830-834 (2004).
- [43] J. Neyton and C. Miller, Discrete Ba<sup>2+</sup> block as a probe of ion occupancy and pore structure in the high-conductance Ca<sup>2+</sup> activated K<sup>+</sup> channel, *J. Gen. Physiol.* **92**, 569-596 (1988).
- [44] M. LeMasurier, L. Heginbotham, and C. Miller, KcsA: It's a potassium channel, *J. General Physiol.* **118**, 303-314 (2001).
- [45] C. M. Nimigean and C. Miller, Na<sup>+</sup> block and permeation in K<sup>+</sup> channel of known structure, *J. Gen. Physiol.* **120**, 323-325 (2002).
- [46] T. J. Dolinsky et al., PDB2PQR: expanding and upgrading automated preparation of biomolecular structures for molecular simulations, *Nucleic Acids Res.* **35**, W522-W525 (2007).
- [47] B. Mallik, A. Masunov, and T. Lazaridis, Distance and exposure dependent effective dielectric function, *J. Comput. Chem.* **23**, 1090-1099 (2002).
- [48] M. Valiskó and D. Boda, Unraveling the behavior of the individual ionic activity coefficients on the basis of the balance of ion-ion and ion-water interactions, *J. Phys. Chem. B* **119**, 1546-1557 (2015).
- [49] J.-L. Liu, H.-j. Hsieh, and B. Eisenberg, Poisson-Fermi modeling of the ion exchange mechanism of the sodium/calcium exchanger, *J. Phys. Chem. B* **120**, 2658-2669 (2016).